# Mathematical Modeling of Gas-solid Flow in Turbine Reactor

Sun Y. Lin Y.L. Zhao K. Lu Y.W.
Chinese Academy of Agricultural Mechanization Sciences, 82# No1. Beishatan Deshengmen wai ,Beijing, China
sunyun@caams.org.cn, linyaling@caams.org.cn, zk@caams.org.cn,luyanwen@sohu.com

**ABSTRACT**

Mathematical models were developed to describe the inner flow field of the turbine reactor. And the models were solved with CFD commercial software. Thus the distributions of the parameters of the flow in the turbine reactor were gained. It was the first time to use CFD technology in the field of turbine reactor and the instruction theory for the study of flow field and the working principles of turbine reactor were provided, the reference for designing and optimizing of the turbine reactor was also offered.

**Key words:** Turbine reactor, modeling, CFD, gas-solid

## 1. INTRODUCTION

High-energy efficiency turbines are important machines for producing modified starch with the dry modified technology. In the reactor there are two kinds of flows--solid and gas flow. Due to the technical complexities and the difficulty in precisely measuring the gas-solid flow field and mass and heat transfer in turbine reactor, many subjects such as modern mathematical methods, hydrodynamics information, CFD knowledge and computer technology have been used to simulate the flow field in turbine reactor(Sun, 2003; Yao, 2002). From the simulation of the flow field, the mass and heat transfer conditions and the complex reactions could be described. The theoretical basis for the design of the turbine reactor was provided. The main objectives of the paper were to develop the mathematical models, solve the equations and gain an understanding of the distribution of parameters of the gas-solid flow.

## 2. DEVELOPMENT OF MATHEMATICAL MODELS

### 2.1 Mathematical Models Development

Mathematical models were developed based on Navier-Stokes equations. Turbulence models, multi-phase flow models, combustion and chemical reaction flow models, free surface flow models and non-Newton fluid models were also used to simulate the flow field (Zhou, 1990). These models were added some additional sources items to transport equation and relation formulation (Virag, 1989). The additional source items will cause non-converging equations. So they must be applied to suitable turbulence models. Currently, many turbulence model are available such as κ-ε standard turbulence model ,ASM( the Algebraic stress model) model, RSM( the Reynolds stress model) model, RNG( the Renormalisation group model) model or the κ - ω turbulence model(Shigeru and David,1984, Bandrowski,1978).

Since the RNG turbulence models have advantages in improving the fluid flow with strong spin and high curvature flow lines, it was used to simulate gas movement in this study. Grain Orbit Model was used to simulate the solid flow.

### 2.2 Discretizing the District

The object simulated in the paper is the gas-solid fluid flow. Therefore the simulation district is the inner part of the turbine reactor. Gambit 2.0 software was used to generate the grid in

this paper (Zhong, 2003). Because the geometry model was very complex, half of the whole machine was calculated in this simulation. Three-dimensional non-frame grid was adopted to discretize the district. Figure.1 showed the non-structure grid that was adjusted and optimized several times by using interleaving grid system in the turbine reactor. In the partition of the grid it considered to encrypt the mesh number in the neighborhood of the cotyledon. The grid amounts to 250000 mesh nodes.

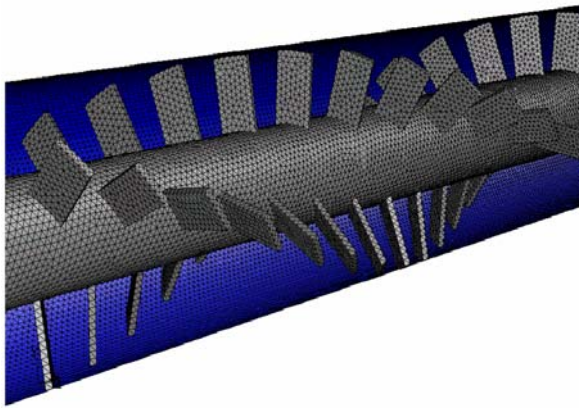

Figure.1 Non-structure grid in turbine reactor

### 2.3 Boundary and Initial conditions

**Inlet boundary conditions of the gas:**

$u_s = 0, v_s = 0, w_s = 40m/s, T_s = 413K, Y_s = 0.025kg/kg$

**Inlet boundary conditions of the solid:**

$u_P = 0, v_P = 0.005m/s, w_P = 0, T_P = 293K, n_p = 0.25kgH_2O/kg$

**Inlet solid material:**

Potato starch , 25% moisture content, 0.056% HCl (quality percent content), the diameter of the starch grain is about 2μm-120μm and the $D_{50}$ is 36μm, the density of the starch material is $\rho = 920\text{kg/m}^3$, the specific heat of the starch material is $C_P = 1250\text{J/kg}\cdot\text{K}$, the coefficient of the heat transferring is $\alpha = 0.08\times10^{-6} m^2/s$.

**Mass flux of the solid material:**

The potato starch was fed into the reactor by screw feeding machine in the tangential direction. It is uniform entrance condition and the intake velocity is $v_{in} = Q_{in}/S_{in}$. Here $Q_{in}$ is the inlet flux and $S_{in}$ is the section area. $Q_{in}$＝0.042kg/s and $v_{in}$＝5.35kg/m$^2$s. So at the entrance the flow velocity of the starch material is $v_0$＝0.057m/s.

**Outlet boundary conditions:**

The outlet pressure is the zero comparing to the atmospheric pressure, that is to say it has no additional pressure action. At the outlet the second boundary conditions was adopted. At the point x=L:

$\partial\phi/\partial x = 0(\phi = u_s, v_s, w_s, k_s, \varepsilon_s, T_s, Y_s)$, $\partial\phi_P/\partial x = 0(\phi_P = u_P, v_P, w_P, k, \varepsilon, T_P, \rho_P, k_P, n_p)$

**Fixed wall:**

Fixed wall, no slippage. Standard wall function was adopted at the near wall area. It had heat transfer between the fixed wall and the external environment.

**Circumvolve boundary condition:**

The laminas on the axis were considered as the circumvolve boundary. The rotate velocity of the lamina was the same as the axis. The rotate speed of the axis was1100rpm and the rotate speed of the out wall was zero. The lamina is insulated. Figure 2 shows the boundary conditions.

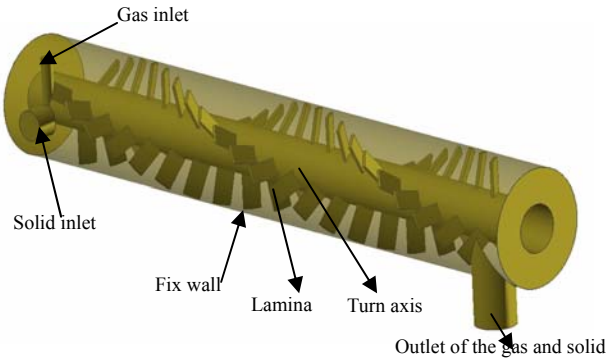


Figure 2 Boundary Condition

### 2.4 Solution of the Models

The control volume method was adopted when the models were solved with mathematical method (Wu, 2002). Non-structure grid and one rank upwind differencing scheme were used to discretize the equations. And then $p-v$ revised SIMPLE arithmetic and TDMA method were used to solve the equations gradually (Wei, et al., 2003).

## 3. Results and Discussions

Three kinds of the installing angle of the lamina $0^o$, $15^o$ and $30^o$ and two kinds of oil temperature 413K and 438K up to six conditions were simulated. The angle was between the lamina plane and the radial plane.

### 3.1 Movement Orbit of the Grain in Turbine Reactor

Figure 3, 4 and 5 showed the movement orbit of the grain under different installing angle of the lamina. In the figures different colors stand for different grain diameters.

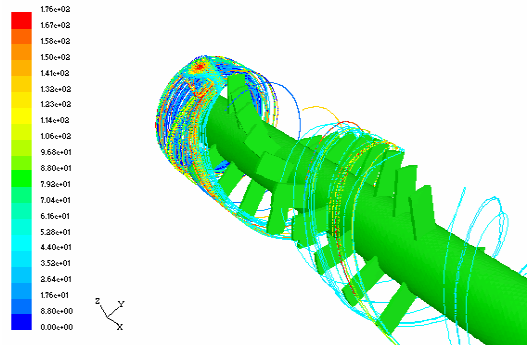

Figure 3 Orbit of the grain in $0^o$ angle

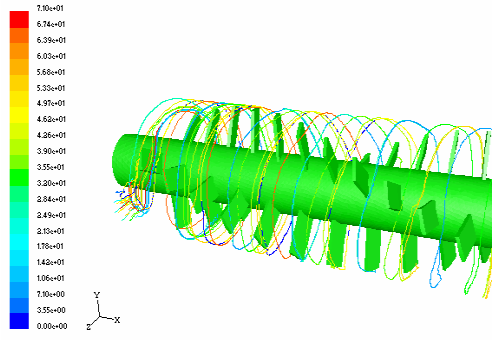

Figure 4 Orbit of the grain in $15^o$ angle

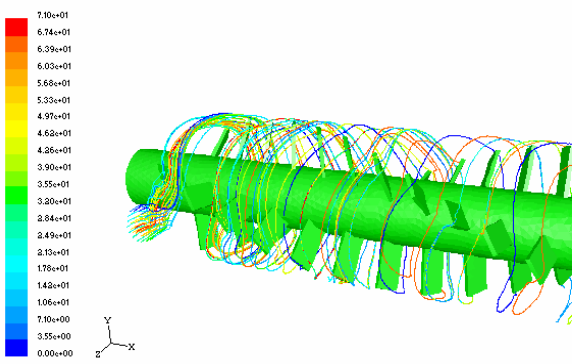

Figure5 Orbit of the grain in 30° angle

Different temperature has little influence on the orbits of the grain. From the figures the orbits of the grain are all continued screw line under each angle. The grain moved along the screw line and all the grain formed a column folium very near the inner wall. The material completed the process of reaction, heat and mass transfer. Different angle has different grain orbit. The main difference is the screw-pitch. It has the largest screw-pitch of 0° angle, larger one of 15° and the least one of 30°. Much larger of the screw-pitch is and much shorter time of the material stays in the dryer and vice versa. So the change of the lamina angle can change the time that the material stays in the turbine reactor. It can reach the requirement of the drying or reacting conditions of varieties of modified starch. From the figure longer drying or reaction time or lower moisture content product need larger installing lamina angle.

### 3.2 Temperature Distribution in Turbine Reactor

In the reaction, providing proper temperature instantly is the most important parameter to reduce the production of the byproduct and improve the production quality. Figure 6 to figure11 showed the distributions of the temperature under different conditions.

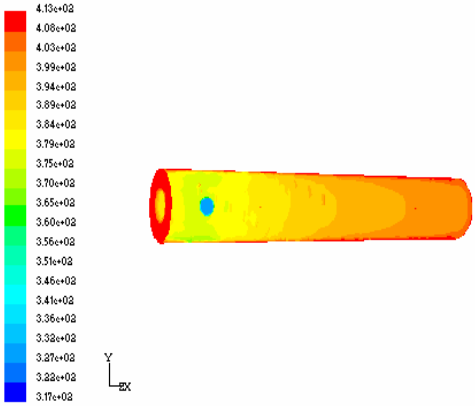

Figure 6 Distribution of the temperature in 0° angle(oil 413K)

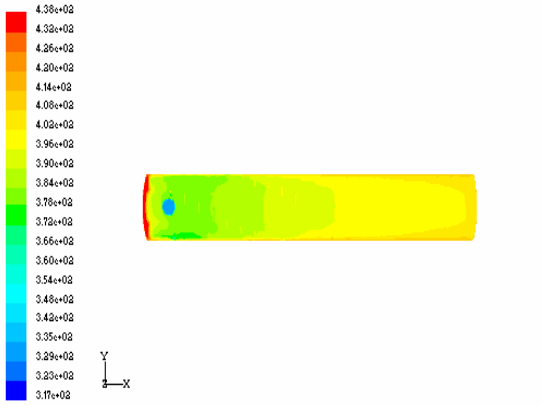

Figure 7 Distribution of the temperature in 0° angle(oil 438K)

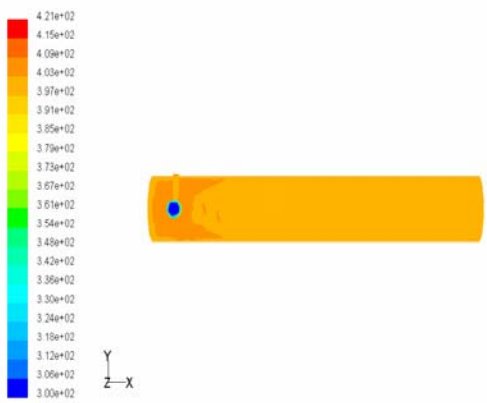

Figure 8 Distribution of the temperature in 15° angle(oil 413K)

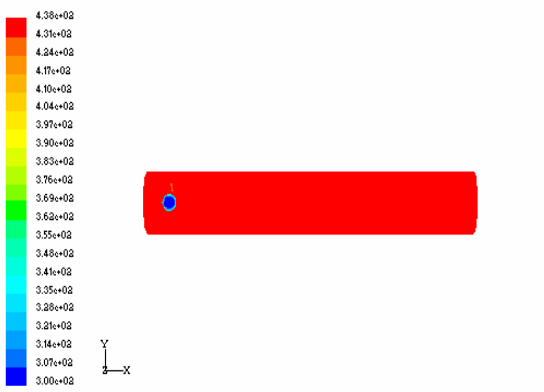

Figure 9 Distribution of the temperature in 15° angle(oil 438K)

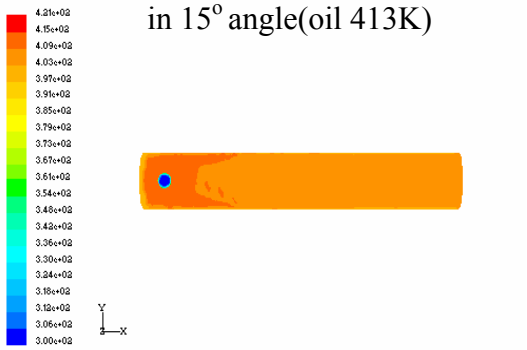

Figure10 Distribution of the temperature in 30° angle(oil 413K)

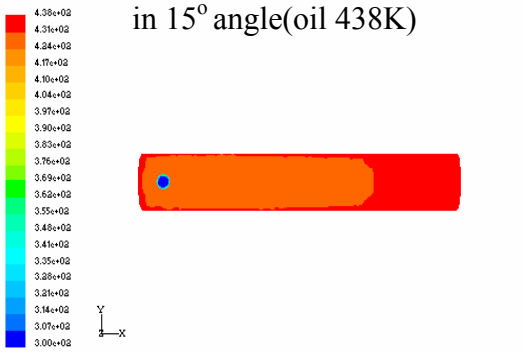

Figure 11 Distribution of the temperature in 30° angle(oil 438K)

The figures showed the temperature distribution of the material flow in the cavity of the reactor. It has the same distribution trend of the three conditions. The temperature increased in the axis direction and it was much lower as the diameter reduced in the radial direction. At the core of the axis the temperature is the lowest and at the nearly inner-wall it is the highest. In the reactor the isothermal plane is a cone surface. This is because the heat transfers to the material near the inner wall by convection and conduction while in the middle of the reactor the main heat transfer method is convection only. From figure 6 and 7 when the angle is 0° the difference of the temperature is much smaller especially in the axis direction under different oil temperatures. The outlet temperatures were about 400K and 405K. Because under 438K oil temperature it would provide more energy for reaction, the reaction would be much more severity and absorb much more energy. The temperature of the outlet would be the same. From the figure 8~11 the temperature distribution trend is much the same under different installing angles of 15° and 30°. When the material with the environment temperature entered it could reach a high temperature quickly at short distance from the inlet. It showed that in such short distant violent heat exchange would have been taken place. When the material goes on the temperature changes are very few and the heat provided by hot wall is mainly used for the reaction of the material. Considering the combination of the temperature distribution and grain movement orbit, the material goes along the screw line near the inner wall. When the screw-pitch is short the exchange time would be longer. The material exposes to such hot flow with such thin layer so it would be easy to reach reaction condition. The installing lamina of 15° and 30° are more favorable for the reaction. From the above analysis different oil temperatures and installing angles of the lamina could be fit for

the reaction of different starches to modify their characteristics.

### 3.3 Distribution of the Velocity of Continued Material

Figure 12 to 35 showed the distribution of the velocity magnitude, tangential velocity, axial velocity, radial velocity magnitude of the continued material under different conditions. Different colors stand for different velocity magnitudes.

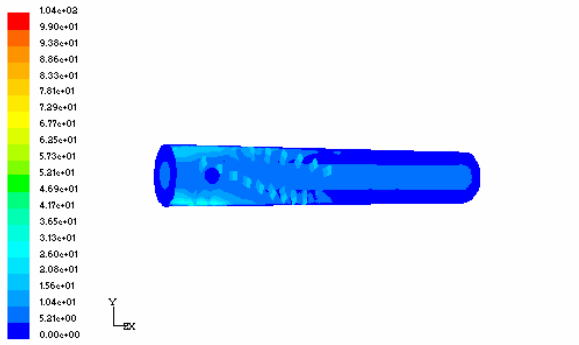

Figure 12 Distribution of the velocity in $0^o$ angle(oil 413K)

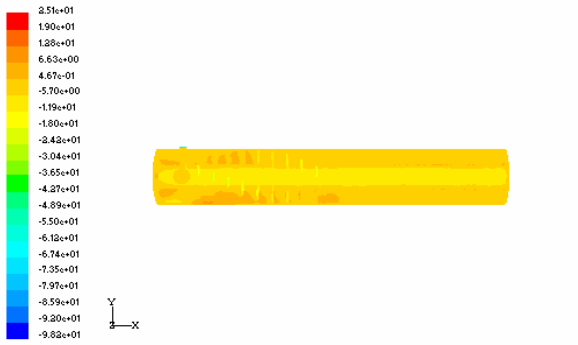

Figure 13 Distribution of the tangential velocity in $0^o$ angle(oil 413K)

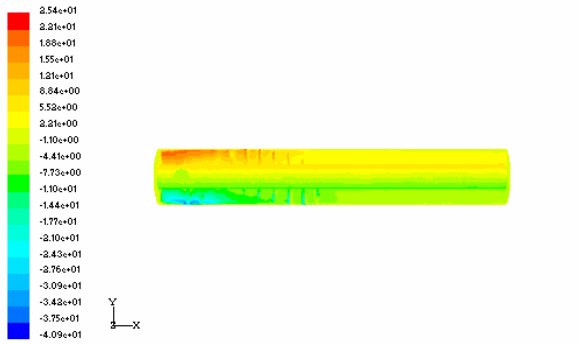

Figure 14 Distribution of the axial velocity in $0^o$ angle(oil 413K)

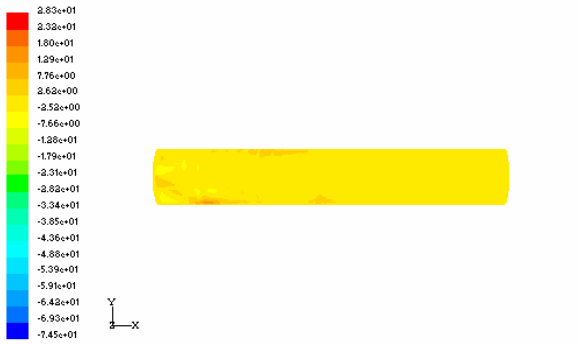

Figure 15 Distribution of the radial velocity in $0^o$ angle(oil 413K)

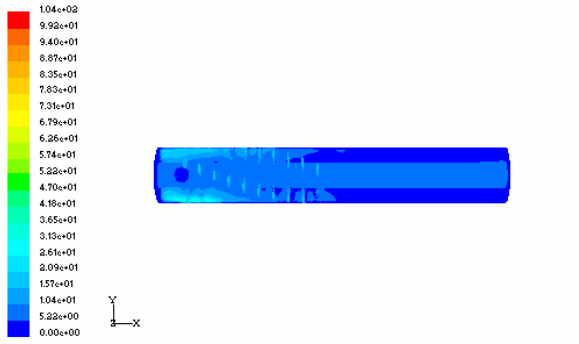

Figure 16 Distribution of the velocity in $0^o$ angle(oil 438K)

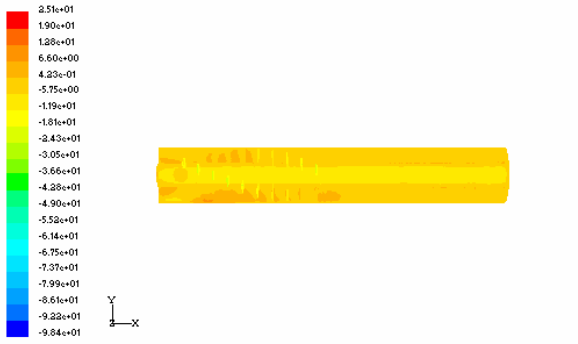

Figure 17 Distribution of the tangential velocity in $0^o$ angle(oil 438K)

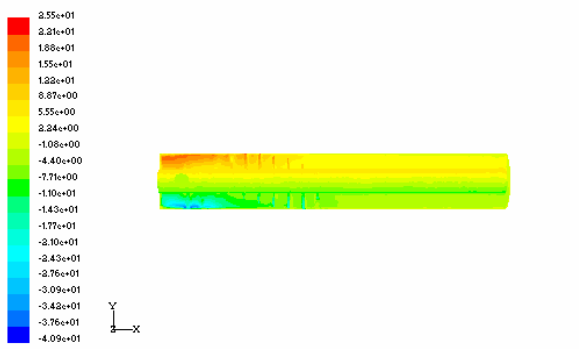

Figure 18 Distribution of the axial velocity in 0° angle(oil 438K)

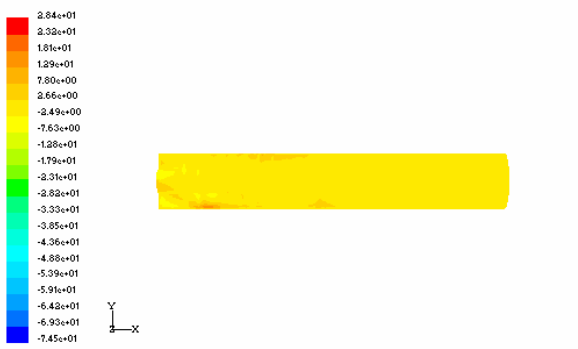

Figure 19 Distribution of the radial velocity in 0° angle(oil 438K)

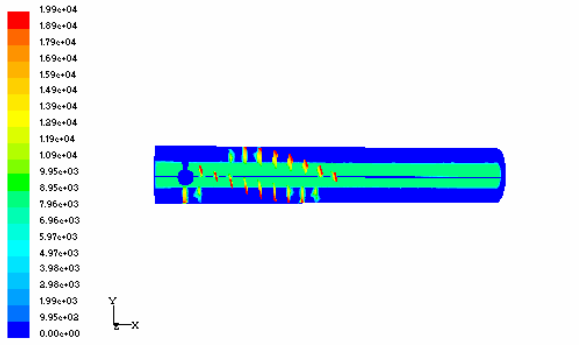

Figure 20 Distribution of the velocity in 15° angle(oil 413K)

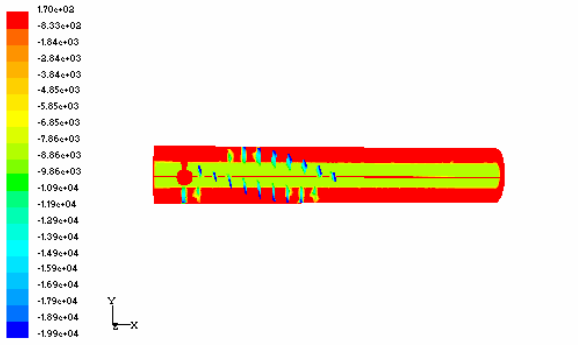

Figure 21 Distribution of the tangential velocity in 15° angle(oil 413K)

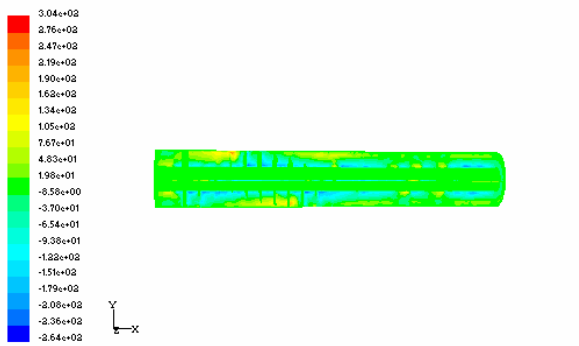

Figure 22 Distribution of the axial velocity in 15° angle(oil 413K)

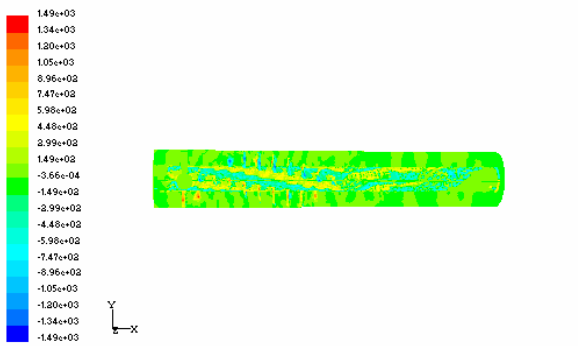

Figure 23 Distribution of the radial velocity in 15° angle(oil 413K)

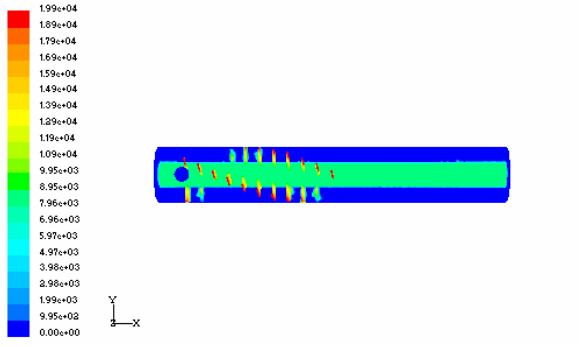

Figure 24 Distribution of the velocity in 15° angle(oil 438K)

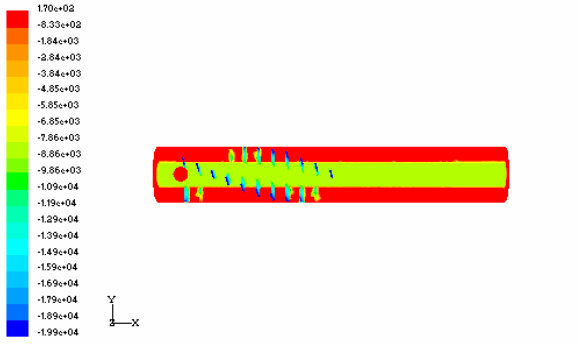

Figure 25 Distribution of the tangential velocity in 15° angle(oil 438K)

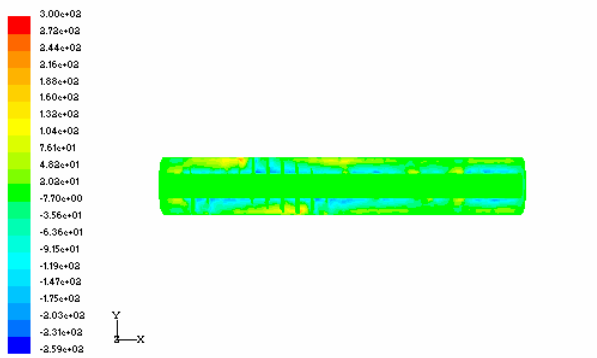

Figure 26 Distribution of the axial velocity in 15° angle(oil 438K)

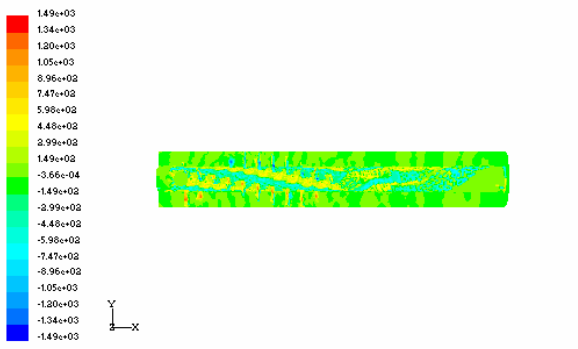

Figure 27 Distribution of the radial velocity in 15° angle(oil 438K)

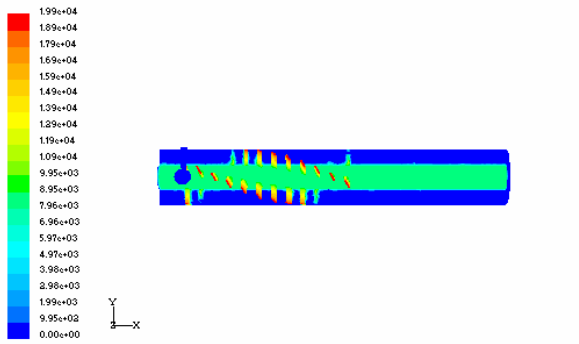

Figure 28 Distribution of the velocity in 30° angle(oil 413K)

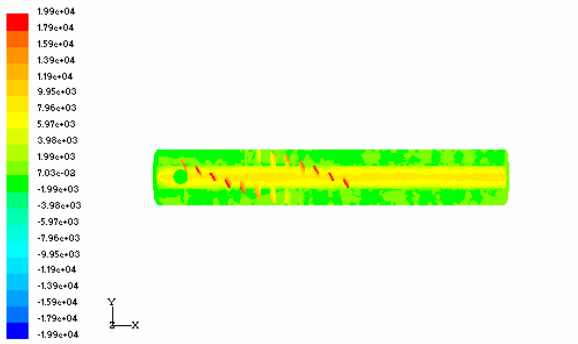

Figure 29 Distribution of the tangential velocity in 30° angle(oil 413K)

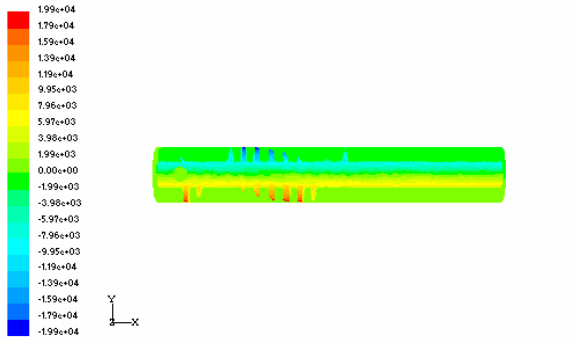

Figure 30 Distribution of the axial velocity in 30° angle(oil 413K)

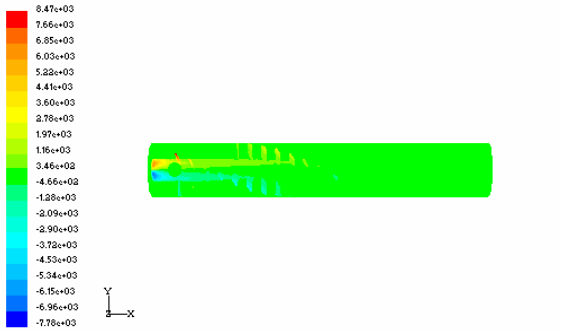

Figure 31 Distribution of the radial velocity in 30° angle(oil 413K)

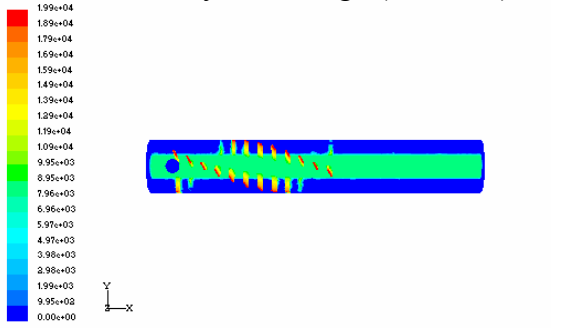

Figure 32 Distribution of the velocity in 30° angle(oil 438K)

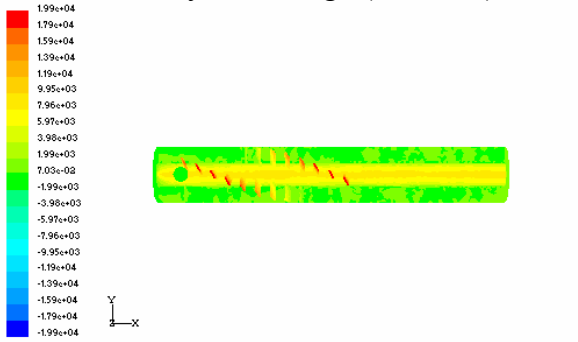

Figure 33 Distribution of the tangential velocity in 30° angle(oil 438K)

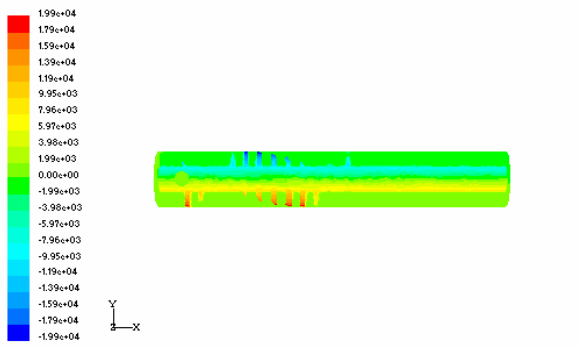


Figure 34 Distribution of the axial velocity in 30° angle (oil 438K)

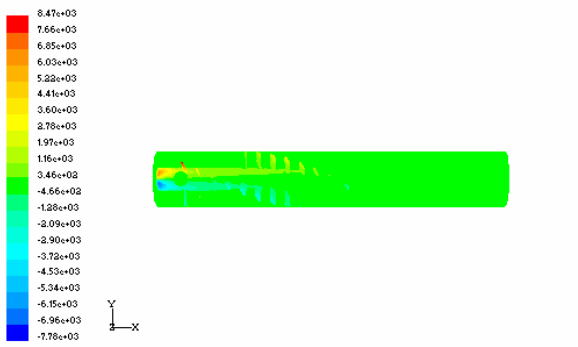


Figure 35 Distribution of the radial velocity in 30° angle (oil 438K)

Figure 12 to 19 show the distribution of the velocity under the installing lamina angle of 0°. The velocity of the solid material increased immediately when combined with the gas at the entrance. The magnitude of synthesizing velocity has the obvious grads along the turbine radial direction. The velocity is bigger at the near wall and it reached 40~70 m/ s. The tangential velocity has the same trend as the synthesize velocity. The figures showed obviously that the larger radius of the lamina was, the bigger the speed was and at the nearly vicinity of the inside-wall the velocity is close to 6m/s. The axial velocity reached the highest at the entrance where the solid material and the gas combined together. And then it slowed down. The highest speed would be 40m/s. The radial velocity had little change and it was about zero except near the wall. From the figures the oil temperature has little influence on the velocity.

Figure 20 to 27 showed the distribution of the velocity under the installing lamina angle of 15°. The synthesize velocity had the obvious grads. At the end of the lamina the velocity is the biggest. The grains moved along inner screw line and form a dynamical thin layer. The velocity reduced rapidly in the radial direction. The tangential velocity has the same trend as the synthesize velocity. The axial velocity is higher at the near wall while at the other location such as the near surface of the lamina it is very low. The radial velocity is higher at the core and at other location it is much lower. The temperature has little influence on the velocity.

Figure 28 to 35 showed the distribution of the velocity under the installing lamina angle of 30°. The synthesize velocity has the same trend as the situation of the installing lamina angle 15°. Just the velocity at the end of the lamina is much higher. The tangential velocity has the same trend as the synthesize velocity. The axial velocity is higher at the end of the lamina while at the core of the axis the speed is nearly zero. The radial velocity is very low so it is always neglected. The temperature has little influence on the velocity.

From the above analysis, the distribution of the velocity has the same trend under the different six conditions. The installing angles are chosen according to the requirement of modified conditions. In the reaction we can regulate reaction time in the reactor and the oil temperature to control the reaction degree and drying degree. It provides the theory instruction for the practical production and optimizing of the design.

### 3.4 Distribution of the Turbulence Intensity of Continued Material

Figure 36 to 41 showed the distribution of the turbulence intensity of the continued material under different conditions.

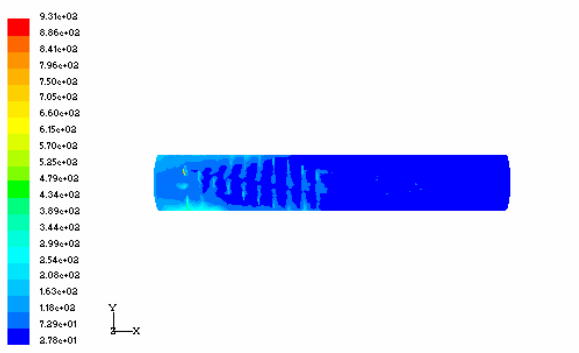

Figure 36 Distribution of the turbulence intensity in 0° angle(oil 413K)

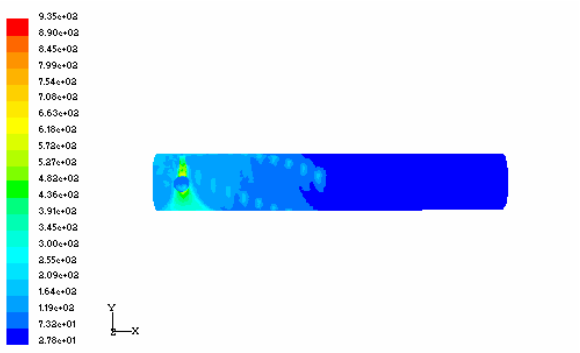

Figure 37 Distribution of the turbulence intensity in 0° angle(oil 438K)

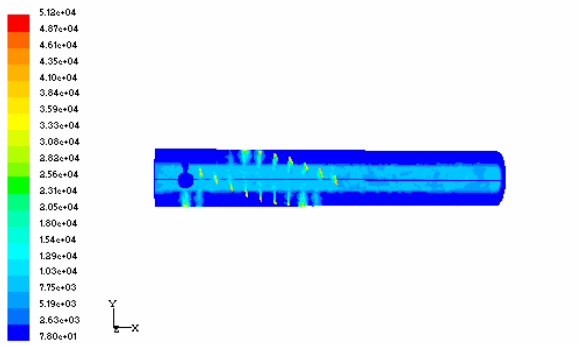

Figure 38 Distribution of the turbulence intensity in 15° angle(oil 413K)

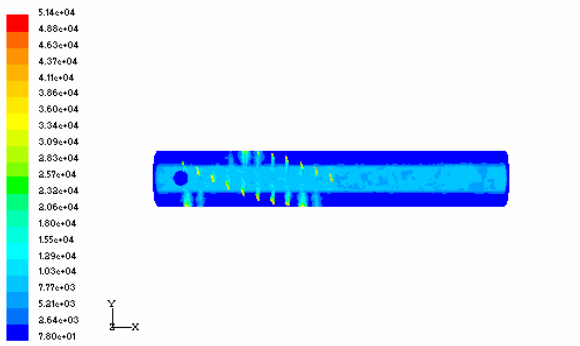

Figure 39 Distribution of the turbulence intensity in 15° angle(oil 438K)

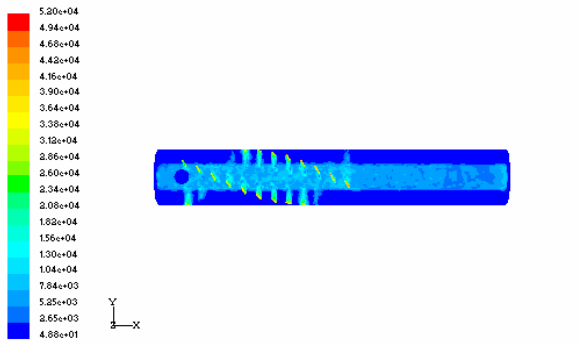

Figure 40 Distribution of the turbulence intensity in 30° angle(oil 413K)

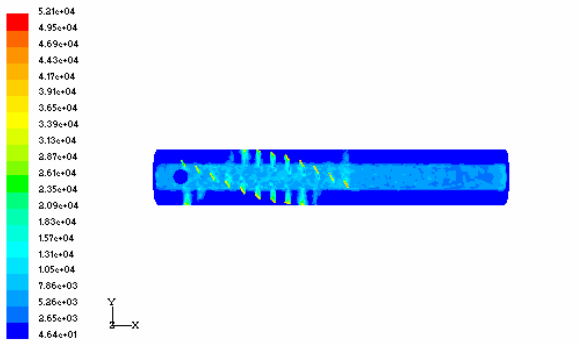

Figure 41 Distribution of the turbulence intensity in 30° angle(oil 438K)

From the above figures, the temperature has little influence on the turbulence intensity while the angles have obvious impact on them. The turbulence intensity of 15° and 30° is about one hundred multiples larger than that of 0°. This is because the change of the angle will change the forces acting on the gases and enhance the turbulence intensity, especially at the end of the lamina. High turbulence intensity prohibits the adherence to the inside-wall. Meanwhile the turbulence increases the reaction probability of the material and chemical reagent.

## 4. CONCLUSIONS

From the simulation results the following conclusions can be drawn:

- The materials moved along the screw line inner the turbine reactor and formed a dynamical column thin layer at the near inside-wall. The screw orbit has relation with the installing angle of the lamina. Regulating the angle can control the resorting time staying in the reactor of the grain. The outer oil temperature has litter influence on the movement orbit.
- The temperature inner the reactor has obvious temperature grads in the axial and radial direction. When the angle is small and the temperature is low it is difficult to reach the required reaction conditions and vice versa. The proper temperature of the oil and installing angle of the lamina were important for producing modified starch.
- The angle has obvious effect on the distribution of the velocity but the temperature of the oil has little influence on it. Under different condition the distribution of tangential velocity, radial velocity and axial velocity have the same regulation. It provides the instruction for practical reacting and drying.
- It has intense turbulence–revolve movement inner the turbine reactor. High turbulence helps to prohibit the adherence to the inside-wall. At the same time it can increase the reaction probability.

## 5. REFERENCES


Chen J.N. Principles of Transfer. *Beijing: Chemistry Industry Publishing House*,2004.Book.

Shigeru Matsumoto, David C.T.PEI. A mathematical analysis of pneumatic drying of grain—I. constant drying rate. Int.J. *Heat Mass Transfer*,1984,127(6):843~849.

Sun H.,Pan J.Z.,Cheng G.. CFD analysis and contrast of some software on the mixing equipment. *Transaction of Institute of Technology of East China*,2003,29(6):625.

Sun H., Keener H., Deng W. and Michel F., Jr. *Development and Validation of 3-D CFD Models to Simulate Airflow and Ammonia Distribution in a High-Rise Hog Building during Summer and Winter Conditions.* Manuscript BC 04 004. Vol. VI. December 2004

Bandrowski, J. G.kaczmrzyk. Gas-to-partical heat transfer in vertical pneumatic conveying of granular materials. *Chem.* Eng. Sci., 1978, 33:1303~1310.

Zhou L.X., Soo. S.L Gas-solid flow and collection of solids in cyclone separator. *Powder Technology* 1990, 63:45~54.

Virag T. Simulation of continuous drying processed by integral equations. *Chem.*Eng. Sci., 1989,44(7):1529~1538.

Wei Z.J., Xu S.,Yuan Y.J., *et al*.. CFD Simulation of Hydrodynamic Characteristics in Stirred Reactors Equipped with Standard Rushton or 45º-Upward PBT Impeller. *Chinese J.Chem*.Eng.,2003,11(4):467.

Wu Z.H.. Simulation of Pulse-active Combustion Spray Drying Process. :*[Master's degree paper].Beijing: China Agricultural University*, 2002.

Yao Z.,Chen K.M.. Summarize of CFD software. *Transaction of Institute of Technology of Shanghai*.2002,24(2):137.

Zhong L., Huang X.B., Jia Z.G. CFD simulation of the critical suspending rotate velocity off bottom of the granules in the Solid-liquid mixing trough. *Transaction of Beijing Chemistry Industry University,*2003,30(6):18.